Resonant response to temperature modulation for enzymatic dynamics characterization

H. Berthoumieux,[1,2] C. Antoine,[2] L. Jullien,[1] and A. Lemarchand[2,*]

[1]*Ecole Normale Supérieure, Département de Chimie, UMR 8640 CNRS ENS UPMC-Paris 6 PASTEUR, 24, rue Lhomond, 75231 Paris Cedex 05, France*

[2]*CNRS, Université Pierre et Marie Curie-Paris 6, Laboratoire de Physique Théorique de la Matière Condensée, UMR 7600, 4 place Jussieu, case courrier 121, 75252 Paris Cedex, France*

We consider enzymes involved in a three-state Michaelis-Menten kinetics and submitted to well-chosen temperature modulations of small amplitude. From the first-order amplitudes of concentration oscillations, we design a response function that is maximum for targeted values of the chemical relaxation times. This resonant function can be used to screen a large set of enzymes and identify the one governed by the desired kinetics. The method gives access to all the dynamical parameters of the targeted enzyme without resorting to a fit. We show how to estimate the precision of this parameter determination and give some hints for experimental validation.

PACS number(s): 82.39.Fk, 87.19.ln

I. INTRODUCTION

A wide variety of enzymes serve as catalysts in living organisms and their dynamical properties are essential characteristics of the metabolic pathways. Recently, considerable progress has been achieved in the determination of their microscopic structure [1–3]. The synthesis of biomimetic enzymes aims at reproducing the structure of the active site [4] in the hope that the artificial enzymes possess the desired dynamics. However, the dynamical properties are not directly connected with the structure: A small change of structure may lead to a large variation of kinetics. Typically, rate constants may vary over ten orders of magnitude and their determination within an order of magnitude is already very demanding. It is therefore of primary importance to design methods to characterize the dynamics of natural as well as artificial enzymes.

A living cell is a complex mixture of various species engaged in networks of chemical reactions [5–8]. Different experimental methods based on relaxation techniques, such as temperature-jump or concentration-jump methods [9], fluctuation correlation spectroscopy (FCS) [10–13] and fast mixing techniques [14] enable the determination of a rate constant in the framework of linear response theory. Reaction relaxation time is deduced from a fit to an exponential decay model for the concentrations. For complex networks governed by a given, possibly nonlinear, dynamics, theoretical optimization methods based on time series numerical treatment offer an alternative [15,16]. However, these predictions rely on fits too, which limits the precision of the rate constant determination and requires large experimental data sets.
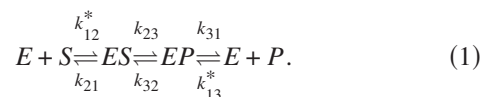
In this paper, we propose a method to characterize the dynamics of enzymes, i.e., three-state linear networks obeying Michaelis-Menten kinetics [8]. The method is based on the resonant response of the enzymatic concentrations to an appropriate periodic excitation. Recently, NaCl concentration oscillations have been used to determine the characteristic times of the limiting processes in a complex network such as

the osmoadaptation pathway of yeast [17]. Here, we choose temperature modulation as a noninvasive perturbation that reveals dynamics [18]. The originality of our approach is to design a resonant function of the dynamical parameters from the enzyme concentrations [19–22], instead of fitting the evolution of the concentrations. It enables us to determine all the dynamical parameters associated with an enzymatic network and to assess the precision of the results.

The paper is organized as follows. In Sec. II, we describe the equilibrium state and dynamics of three-state enzymatic networks. In Sec. III, we analytically determine the amplitude of concentration oscillations due to a small temperature modulation and show the occurrence of a resonance phenomenon when the chemical relaxation time matches the period of the external excitation. Then, for a chosen temperature modulation, we build a function of the dynamical parameters which is maximum for a given dynamics. In Sec. IV, we show how to use this resonant function for the screening of a set of enzymes and for the identification of the one which is the closest to the targeted dynamics. Before concluding, we determine the rate constants of the latter and show how to estimate the precision of the result.

II. EQUILIBRIUM STATE AND DYNAMICS OF A THREE-STATE MICHAELIS-MENTEN KINETICS

We consider an enzyme E, involved in a three-state Michaelis-Menten kinetics, which catalyses the transformation of a substrate S into a product P:

$$E + S \underset{k_{21}}{\overset{k_{12}^*}{\rightleftharpoons}} ES \underset{k_{32}}{\overset{k_{23}}{\rightleftharpoons}} EP \underset{k_{13}^*}{\overset{k_{31}}{\rightleftharpoons}} E + P. \tag{1}$$
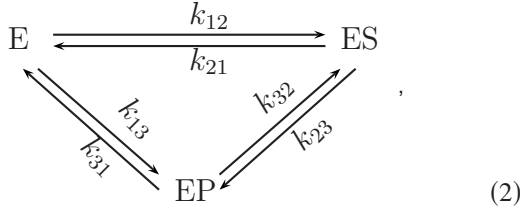
The substrate and product are in great excess with respect to the enzyme so that their concentration S and P can be considered constant. In the enzyme perspective, the reaction is cyclic and unimolecular with three states E, ES, and EP:

TABLE I. Expression of the coefficients κ_{jk}^i ($i=0,1$; $j,k=1,2$), of the matrix $\mathbf{M}^i$ as a function of the zeroth and first-order rate constants k_{lm}^i ($i=0,1$; $l,m=1,2,3$; $l \neq m$).

| κ_{11}^i | $-(k_{12}^i+k_{13}^i+k_{31}^i)$ | κ_{12}^i | $k_{21}^i-k_{31}^i$ |
| κ_{21}^i | $k_{12}^i-k_{32}^i$ | κ_{22}^i | $-(k_{21}^i+k_{23}^i+k_{32}^i)$ |

$$E \underset{k_{21}}{\overset{k_{12}}{\rightleftarrows}} ES$$

$$\quad (2)$$

where $(k_{21},k_{32},k_{23},k_{31})$ are first-order rate constants and $k_{12}=k_{12}^*S$ and $k_{13}=k_{13}^*P$ are pseudo-first-order rate constants. The system is supposed to be in equilibrium at temperature T^0. Consequently, the equilibrium concentrations (E^0,ES^0,EP^0) obey detailed balance:

$$k_{12}^0 E^0 = k_{21}^0 ES^0, \quad k_{23}^0 ES^0 = k_{32}^0 EP^0, \quad k_{31}^0 EP^0 = k_{13}^0 E^0, \tag{3}$$

which implies $\frac{k_{12}^{*0}k_{23}^0 k_{31}^0}{k_{21}^0 k_{32}^0 k_{13}^{0*}} = \frac{P}{S}$, i.e.,

$$\frac{k_{12}^0 k_{23}^0 k_{31}^0}{k_{21}^0 k_{32}^0 k_{13}^0} = 1. \tag{4}$$

The equilibrium state at temperature T^0 is given by the vector

$$\mathcal{E}^0 = \begin{pmatrix} E^0 \\ ES^0 \end{pmatrix} = \begin{pmatrix} \dfrac{1}{1+\dfrac{k_{12}^0}{k_{21}^0}+\dfrac{k_{13}^0}{k_{31}^0}} \\[3ex] \dfrac{1}{1+\dfrac{k_{21}^0}{k_{12}^0}+\dfrac{k_{23}^0}{k_{32}^0}} \end{pmatrix} \tag{5}$$

and the concentration EP^0 is imposed by the conservation relation $E^0+ES^0+EP^0=1$. The linear operator $\mathbf{M}^0$ associated with the dynamics of the enzymatic network is

$$\mathbf{M}^0 = \begin{pmatrix} \kappa_{11}^0 & \kappa_{12}^0 \\ \kappa_{21}^0 & \kappa_{22}^0 \end{pmatrix}, \tag{6}$$

where the coefficients κ_{jk}^0 ($j,k=1,2$) as a function of the rate constants k_{lm}^0 ($l,m=1,2,3$; $l \neq m$), are given in Table I. As a consequence of detailed balance, the matrix $\mathbf{M}^0$ possesses two real and negative eigenvalues (λ_+,λ_-) [23,24]:

$$\lambda_{\pm} = \frac{\kappa_{11}^0 + \kappa_{22}^0}{2} \pm \frac{1}{2}\sqrt{(\kappa_{11}^0+\kappa_{22}^0)^2 - 4(\kappa_{11}^0\kappa_{22}^0 - \kappa_{21}^0\kappa_{12}^0)}. \tag{7}$$

We consider the nondegenerate case where the two eigenvalues are different and obey $\lambda_- < \lambda_+ < 0$.

The usual change-of-basis matrix $\mathbf{P}$, whose jth column is equal to the jth normalized eigenvector of $\mathbf{M}^0$, may be written as

$$\mathbf{P} = \begin{pmatrix} \cos(\theta_+) & \cos(\theta_-) \\ \sin(\theta_+) & \sin(\theta_-) \end{pmatrix}. \tag{8}$$

The "eigenangles" θ_+ and θ_- characterize the eigenvectors, respectively, associated with the eigenvalues λ_+ and λ_-. The expressions of the eigenangles as a function of the rate constants are deduced from the following equations:

$$\tan(\theta_{\pm}) = \frac{\lambda_{\pm} - \kappa_{11}^0}{\kappa_{12}^0}, \tag{9}$$

where the eigenvalues $\lambda_{\pm}$ are given in Eq. (7) and the coefficients κ_{ij}^0 are given in Table I. For enzymes which satisfy detailed balance, the expression of the parameters $\lambda_+,\lambda_-,E^0,ES^0,\theta_+,\theta_-$ as a function of the rate constants k_{ij}^0 can be deduced from Eqs. (5), (7), and (9). Reciprocally, Table II gives the expression of k_{12}^0, k_{23}^0 and k_{31}^0 versus $(\lambda_+,\lambda_-,E^0,ES^0,\theta_+,\theta_-)$. The expressions for the three other rate constants are deduced from mass conservation and from Eq. (3). When use is made of Table II, the relation between the rate constants [Eq. (4)] can be rewritten as

$$E^0(1-E^0)\tan(\theta_+)\tan(\theta_-)$$
$$+ E^0 ES^0[\tan(\theta_+) + \tan(\theta_-)] + ES^0(1-ES^0) = 0 \tag{10}$$

which relates E^0, ES^0, θ_+, and θ_-. Note that the parameters

TABLE II. Expression of the rate constants k_{12}^0, k_{23}^0, and k_{31}^0 versus λ_+, λ_-, E^0, ES^0, θ_+, θ_-. The four parameters E^0, ES^0, θ_+, θ_- obey Eq. (10).

k_{12}^0	$\dfrac{1}{\tan(\theta_-)-\tan(\theta_+)}\{[(1-E^0)\tan(\theta_+)\tan(\theta_-)+ES^0\tan(\theta_+)]\lambda_+ - [(1-E^0)\tan(\theta_+)\tan(\theta_-)$ $+ES^0\tan(\theta_-)]\lambda_-\}$
k_{23}^0	$\dfrac{1}{\tan(\theta_-)-\tan(\theta_+)}\dfrac{1-E^0-ES^0}{ES^0}\{[-E^0\tan(\theta_+)\tan(\theta_-)+ES^0\tan(\theta_+)]\lambda_+ + [E^0\tan(\theta_+)\tan(\theta_-)$ $-ES^0\tan(\theta_-)]\lambda_-\}$
k_{31}^0	$\dfrac{1}{\tan(\theta_-)-\tan(\theta_+)}\{[-E^0\tan(\theta_-)+ES^0]\lambda_+ + [E^0\tan(\theta_+)-ES^0]\lambda_-\}$

(λ_+, λ_-) are decoupled from $E^0, ES^0, \theta_+, \theta_-$. The equilibrium state and dynamics of the enzyme are characterized by six rate constants, five of which are independent and the sixth one is determined by Eq. (4). Equivalently, thermodynamics and dynamics are determined by the following five parameters: the two eigenvalues (λ_+, λ_-) and three of the four parameters $(E^0, ES^0, \theta_+, \theta_-)$.

III. TEMPERATURE MODULATION AND CONCENTRATION OSCILLATIONS

In this section, we determine the effect of a small temperature modulation on the enzyme concentrations. We consider an enzymatic network submitted to a sinusoidal modulation of temperature T, around the temperature T^0 with a small amplitude βT^0 and angular frequency ω:

$$T = T^0[1 + \beta \sin(\omega t)], \quad \beta \ll 1. \tag{11}$$

The angular frequency ω is sufficiently small for thermal equilibrium to be maintained. Following Arrhenius, the rate constants can be written as

$$k_{ij} = r_{ij} \exp\left(-\frac{E_{a,ij}}{RT}\right), \tag{12}$$

where r_{ij} is a pre-exponential factor, R is the individual gas constant, and $E_{a,ij}$ is the activation energy. Taking r_{ij} constant in the relevant temperature range [25–27], we expand the rate constants to the first order in the perturbation and obtain

$$k_{ij}(t) = k_{ij}^0 + \beta k_{ij}^1 \sin(\omega t), \tag{13}$$

where $k_{ij}^0 = r_{ij} \exp(-\epsilon_{ij})$ are the rate constants at temperature T^0 and where

$$k_{ij}^1 = k_{ij}^0 \epsilon_{ij} \tag{14}$$

with $\epsilon_{ij} = \frac{E_{a,ij}}{RT^0}$. According to Eq. (13), the rate constant $k_{ij}(t)$ appears as the sum of an unperturbed value k_{ij}^0 at temperature T^0 and an oscillating term at the angular frequency ω in phase with the temperature to the first order in the perturbation β.

A large set of three-state enzymatic networks leads to a nearly continuous sampling of the independent parameters (r_{ij}, ϵ_{ij}) or, equivalently, of (k_{ij}^0, k_{ij}^1). However, according to Eq. (14), the first order correction k_{ij}^1 is the product of a

linear function of ϵ_{ij} and an exponential function of ϵ_{ij} hidden in k_{ij}^0. In the following, for simplicity, we neglect the linear variation of k_{ij}^1 versus ϵ_{ij} with respect to its exponential variation. It amounts to allocating the same set of ϵ_{ij} to any three-state enzymatic network. Under this approximation, we characterize the equilibrium state and the dynamics of a network submitted to a small temperature modulation by the set of the five rate constants k_{ij}^0 only.

The instantaneous state of an enzymatic network submitted to the temperature modulation of Eq. (11) is given by the vector

$$\mathcal{E}(t) = \mathcal{E}^0 + \beta \mathcal{E}^1(t) = \begin{pmatrix} E(t) \\ ES(t) \end{pmatrix} \tag{15}$$

and the evolution of the system is governed by the equation

$$\frac{d\mathcal{E}(t)}{dt} = \mathbf{M}(t)\mathcal{E}(t) + \mathbf{F}(t), \tag{16}$$

where the matrix $\mathbf{M}(t)$ and the vector $\mathbf{F}(t)$ satisfy $\mathbf{M}(t) = \mathbf{M}^0 + \beta \mathbf{M}^1 \sin(\omega t)$ and $\mathbf{F}(t) = \mathbf{F}^0 + \beta \mathbf{F}^1 \sin(\omega t)$, with

$$\mathbf{M}^i = \begin{pmatrix} \kappa_{11}^i & \kappa_{12}^i \\ \kappa_{21}^i & \kappa_{22}^i \end{pmatrix}, \quad \mathbf{F}^i = \begin{pmatrix} k_{31}^i \\ k_{32}^i \end{pmatrix} \quad \text{for } i = 0, 1. \tag{17}$$

The expression of the coefficients κ_{jk}^i $(j, k = 1, 2)$, of $\mathbf{M}^i$ as functions of the rate constants k_{lm}^i $(l, m = 1, 2, 3; \; l \neq m)$, is given in Table I with k_{lm}^1 obeying Eq. (14). In the eigenvector basis, the dynamical state of an enzymatic network is given by the vector

$$\mathbf{X}(t) = \mathbf{P}^{-1}\mathcal{E}(t) = \mathbf{X}^0 + \beta \mathbf{X}^1(t), \tag{18}$$

where $\mathbf{P}^{-1}$ is the inverse matrix of $\mathbf{P}$ which is defined in Eq. (8). The coordinates $X_\pm^1$ of the vector $\mathbf{X}^1(t)$ are associated with the following uncoupled equations:

$$\frac{dX_\pm^1(t)}{dt} = \lambda_\pm X_\pm^1(t) + \lambda_\pm \alpha_\pm \sin(\omega t), \tag{19}$$

where $\lambda_\pm \alpha_\pm$ are the coordinates of the vector $\mathbf{P}^{-1}(\mathbf{M}^1 . \mathbf{P} . \mathbf{X}^0 + \mathbf{F}^1)$. The coefficients $\alpha_\pm$ depend only on the equilibrium state, the eigenangles $\theta_\pm$ and the standard enthalpies of reaction $\frac{\Delta_{ij}H^0}{RT^0} = \epsilon_{ij} - \epsilon_{ji}$ as follows:

$$\alpha_\pm = - \frac{E^0 ES^0 (1 - E^0 - ES^0)\left\{\tan(\theta_\pm)\dfrac{\Delta_{12}H^0}{RT^0} + [1 + \tan(\theta_\pm)]\dfrac{\Delta_{31}H^0}{RT^0}\right\}}{\cos(\theta_\pm)[E^0(1 - E^0)\tan(\theta_\pm)^2 + 2E^0 ES^0 \tan(\theta_\pm) + ES^0(1 - ES^0)]}. \tag{20}$$

As a consequence of detailed balance, the coefficients $\lambda_\pm \alpha_\pm$ are linear combinations of the standard enthalpies of reaction and they vanish for $\epsilon_{ij} = \epsilon_{ji}$. The system remains in equilibrium in the presence of temperature oscillations, if the three pseudoisomerizations of the network are thermoneutral.

We look for asymptotic solutions of Eq. (19) in the form $X_\pm^1(t) = X_{\pm,\sin}^1 \sin(\omega t) + X_{\pm,\cos}^1 \cos(\omega t)$. It reads

TABLE III. Expression of the first-order amplitudes $E^1_{\sin}(\omega)$, $ES^1_{\sin}(\omega)$ and $E^1_{\cos}(\omega)$, $ES^1_{\cos}(\omega)$ which are, respectively, in phase and out-of-phase with temperature. The expression of $\alpha_\pm$ is given in Eq. (20).

$$E^1_{\sin}(\omega) = -\cos(\theta_+)\frac{\alpha_+\lambda_+^2}{\omega^2+\lambda_+^2} - \cos(\theta_-)\frac{\alpha_-\lambda_-^2}{\omega^2+\lambda_-^2} \qquad ES^1_{\sin}(\omega) = -\sin(\theta_+)\frac{\alpha_+\lambda_+^2}{\omega^2+\lambda_+^2} - \sin(\theta_-)\frac{\alpha_-\lambda_-^2}{\omega^2+\lambda_-^2}$$

$$E^1_{\cos}(\omega) = -\omega\left(\cos(\theta_+)\frac{\alpha_+\lambda_+}{\omega^2+\lambda_+^2} + \cos(\theta_-)\frac{\alpha_-\lambda_-}{\omega^2+\lambda_-^2}\right) \qquad ES^1_{\cos}(\omega) = -\omega\left(\sin(\theta_+)\frac{\alpha_+\lambda_+}{\omega^2+\lambda_+^2} + \sin(\theta_-)\frac{\alpha_-\lambda_-}{\omega^2+\lambda_-^2}\right)$$

$$X^1_{\pm,\sin}(\omega) = -\alpha_\pm\frac{\lambda_\pm^2}{\omega^2+\lambda_\pm^2}, \tag{21}$$

$$X^1_{\pm,\cos}(\omega) = -\alpha_\pm\frac{\omega\lambda_\pm}{\omega^2+\lambda_\pm^2}. \tag{22}$$

Interestingly, the function $|X^1_{\pm,\cos}(\omega)|$, if considered as a function of the eigenvalues $\lambda_\pm$ at fixed angular frequency ω, is maximum for $|\lambda_\pm| = \omega$. In the following, we take advantage of this resonance phenomenon to design a resonant function of the dynamical parameters which characterize a network. The expression of the vector $\mathcal{E}$,

$$\mathcal{E}(t) = \mathcal{E}^0 + \beta[\mathcal{E}^1_{\sin}(\omega)\sin(\omega t) + \mathcal{E}^1_{\cos}(\omega)\cos(\omega t)], \tag{23}$$

is deduced from the vector $\mathbf{X}(t)$ by inverting Eq. (18). The expressions of the in-phase $[E^1_{\sin}(\omega), ES^1_{\sin}(\omega)]$ and out-of-phase amplitudes $[E^1_{\cos}(\omega), ES^1_{\cos}(\omega)]$ of the concentrations are given in Table III.

IV. DESIGN OF A RESONANT RESPONSE FUNCTION

Our goal is to design a protocol to determine which enzymatic network, among a collection of three-state Michaelis-Menten networks, possesses a desired kinetics, i.e., a set of targeted dynamical parameters $(\lambda_\pm^R, \theta_\pm^R)$. Our strategy is to use the response of enzymatic networks to a temperature modulation to reveal their dynamics and to build a function $R(\lambda_\pm, E^0, \theta_\pm)$ from the out-of-phase amplitudes $[E^1_{\cos}(\omega), ES^1_{\cos}(\omega)]$ of the concentration oscillations, which are supposed to be experimentally accessible. The response R is a function of the thermodynamical and dynamical parameters $(\lambda_\pm, E^0, \theta_\pm)$, ES^0 being deduced from detailed balance, as expressed in Eq. (10). The function $R(\lambda_\pm, E^0, \theta_\pm)$ is devised to be maximum for the so-called resonant dynamical values $(\lambda_\pm^R, \theta_\pm^R)$ that can be chosen at will. The existence of a maximum of the out-of-phase coordinates $X^1_{\pm,\cos}(\omega)$ for $|\lambda_\pm| = \omega$ prompts us to choose the following temperature modulation at the two targeted eigenfrequencies $|\lambda_+^R|$ and $|\lambda_-^R|$:

$$T = T^0[1 + \beta\sin(|\lambda_+^R|t) + \beta\sin(|\lambda_-^R|t)]. \tag{24}$$

Then, the dynamical state of an enzymatic network is given by the vector

$$\mathcal{E}(t) = \mathcal{E}^0 + \beta[\mathcal{E}^1_{\sin}(|\lambda_+^R|)\sin(|\lambda_+^R|t) + \mathcal{E}^1_{\cos}(|\lambda_+^R|)\cos(|\lambda_+^R|t) \tag{25}$$

$$+ \mathcal{E}^1_{\sin}(|\lambda_-^R|)\sin(|\lambda_-^R|t) + \mathcal{E}^1_{\cos}(|\lambda_-^R|)\cos(|\lambda_-^R|t)]. \tag{26}$$

We project the out-of-phase amplitude vector $\mathcal{E}^1_{\cos}(\omega)$ onto the resonant eigendirections using the inverse matrix of $\mathbf{P}^R$, which is deduced from Eq. (8) for the targeted eigenangles $\theta_\pm^R$. We obtain the vector

$$\mathbf{S}(\omega) = (\mathbf{P}^R)^{-1}\mathcal{E}^1_{\cos}(\omega) \tag{27}$$

whose coordinates $S_+(\omega)$ and $S_-(\omega)$ are the projection of the vector $\mathcal{E}^1_{\cos}(\omega)$ onto the targeted eigendirections defined by the eigenangles θ_+^R and θ_-^R. When excited at the targeted eigenfrequency $|\lambda_+^R|$ ($|\lambda_-^R|$), the coordinate $S_+(\omega)$ [$S_-(\omega)$] is expected to be maximum if the dynamical parameters $(\lambda_\pm, \theta_\pm)$ match the targeted dynamical parameters. Then, to increase the sensitivity, we define the response function as the following product:

$$R(\lambda_\pm, E^0, \theta_\pm) = |S_+(|\lambda_+^R|)||S_-(|\lambda_-^R|)|$$
$$= \frac{1}{(\sin(\theta_-^R - \theta_+^R))^2}|\sin(\theta_-^R)E^1_{\cos}(|\lambda_+^R|)$$
$$- \cos(\theta_-^R)ES^1_{\cos}(|\lambda_+^R|)||-\sin(\theta_+^R)E^1_{\cos}(|\lambda_-^R|)$$
$$+ \cos(\theta_+^R)ES^1_{\cos}(|\lambda_-^R|)|. \tag{28}$$

When use is made of the expression of the first-order amplitudes $E^1_{\cos}(\omega)$ and $ES^1_{\cos}(\omega)$ given in Table III, the expression of the response function $R(\lambda_\pm, E^0, \theta_\pm)$ can be rewritten as

$$R(\lambda_\pm, E^0, \theta_\pm) = \frac{\lambda_+^R\lambda_-^R}{\sin(\theta_-^R - \theta_+^R)^2}\left|\alpha_+\sin(\theta_-^R - \theta_+)\frac{\lambda_+}{(\lambda_+^R)^2 + \lambda_+^2}\right.$$
$$\left. - \alpha_-\sin(\theta_-^R - \theta_-)\frac{\lambda_-}{(\lambda_+^R)^2 + \lambda_-^2}\right|$$
$$\times\left|\alpha_+\sin(\theta_+ - \theta_+^R)\frac{\lambda_+}{(\lambda_-^R)^2 + \lambda_+^2}\right.$$
$$\left. - \alpha_-\sin(\theta_- - \theta_+^R)\frac{\lambda_-}{(\lambda_-^R)^2 + \lambda_-^2}\right|. \tag{29}$$

We conjecture that the function $R(\lambda_\pm, E^0, \theta_\pm)$ is maximum for

$$\lambda_\pm \approx \lambda_\pm^R, \tag{30}$$

$$\theta_\pm \approx \theta_\pm^R, \tag{31}$$

provided the dynamics of the resonant enzymatic network is given by the nondegenerate topology of Eq. (2). In particular, the conjecture requires that

$$E^0 \neq 1, \quad ES^0 \neq 1, \quad EP^0 \neq 1, \quad \lambda_+^R \neq \lambda_-^R, \quad |\theta_\pm^R| \neq \pi/2. \tag{32}$$

For instance, the case $|\theta_\pm^R| = \pi/2$ leads to uncoupled variables E and ES and not to a "triangle-type" mechanism.

The dependence of $R(\lambda_\pm, E^0, \theta_\pm)$ on the angles $\theta_\pm$ in the prefactors of the Lorentzian functions of $\lambda_\pm$ is complicated, which makes difficult the use of the analytical expression of the maximum. Consequently, we begin with a numerical proof of the result announced in Eq. (31) for the eigenangles. To this goal, we compute the values of the response function $R(\lambda_\pm, E^0, \theta_\pm)$ for a large number of enzymatic networks. Each sampled network is actually defined by five rate constants, for example, $k_{12}^0, k_{21}^0, k_{23}^0, k_{32}^0, k_{31}^0$. The remaining rate constant k_{13}^0 is imposed by detailed balance (4). The values of the enthalpies of reaction $\Delta_{12}H^0$, $\Delta_{23}H^0$, and $\Delta_{31}H^0 = -\Delta_{12}H^0 - \Delta_{23}H^0$ are supposed to be the same for all the generated networks. We choose a targeted enzymatic network which is associated with the rate constants $k_{12}^{0,R}, k_{21}^{0,R}, k_{23}^{0,R}, k_{32}^{0,R}, k_{31}^{0,R}$ or, equivalently, with the dynamical parameters $(\lambda_\pm^R, \theta_\pm^R)$ deduced from Eqs. (7) and (9) and the equilibrium state E^{0R}, ES^{0R} deduced from Eq. (5). We generate a uniform sampling in logarithmic scale for the rate constants $k_{12}^0, k_{21}^0, k_{23}^0, k_{32}^0, k_{31}^0$ around the targeted values which leads to a nonuniform sampling of the eigenvalues $\lambda_\pm$, eigenangles $\theta_\pm$, and equilibrium concentration E^0. The value of the equilibrium concentration ES^0 is imposed by Eq. (10).

Each generated network is submitted to the two-frequency temperature modulation given in Eq. (24). Table III is used to compute the out-of-phase amplitude of the concentration oscillations $E_{\cos}^1(|\lambda_\pm^R|)$ and $ES_{\cos}^1(|\lambda_\pm^R|)$. Then, we calculate the matrix $(\mathbf{P}^R)^{-1}$ by inverting Eq. (8) for $\theta_\pm = \theta_\pm^R$ and compute the values of the response function $R(\lambda_\pm, E^0, \theta_\pm)$ for each network, according to Eq. (28). In order to check the validity of the conjecture, we have investigated the behavior of $R(\lambda_\pm, E^0, \theta_\pm)$ as a function of $\theta_\pm$ for many choices of targeted dynamics. Figures 1 and 2 give representative results. Due to the projection of the five-variable function $R(\lambda_\pm, E^0, \theta_\pm)$ onto a one-dimensional space, the points appearing in Figs. 1 and 2 fill up the curves. As conjectured, the response function has a maximun for $\theta_\pm^{\max} \approx \theta_\pm^R$. As seen in Fig. 1, the agreement between the angle $\theta_-^{\max}$, which is associated with the maximum of $R(\lambda_\pm, E^0, \theta_\pm)$, and the targeted eigenangles θ_-^R is excellent. For this choice of the resonant parameters, the discrepancy between $\theta_+^{\max}$ and θ_+^R is larger. To quantify this discrepancy, we define a distance d_θ as $d_\theta = |\frac{\theta_+^{\max} - \theta_+^R}{\pi/2}|$. Such a definition takes into account the periodicity of $R(\lambda_\pm, E^0, \theta_\pm)$ as a function of the eigenangle, which implies that the discrepancy cannot exceed $\pi/2$. As shown in Fig. 2, the discrepancy between the angle which is associated with the maximum of $R(\lambda_\pm, E^0, \theta_\pm)$ and the targeted eigenangle can reach 20%.
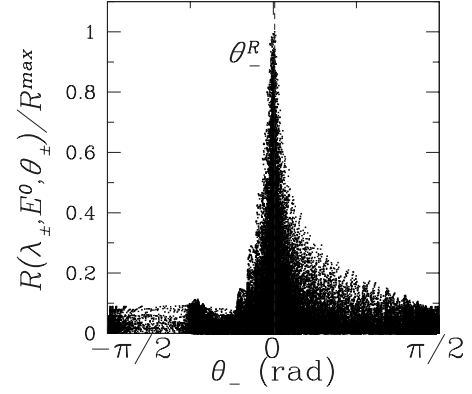

FIG. 1. Normalized response $R(\lambda_\pm, E^0, \theta_\pm)/R^{\max}$ versus eigenangle θ_- for enzymatic networks with three states. The figure is plotted by using Eqs. (29), (37), and (9) to compute the response function and the eigenangle θ_- from a uniform sampling of five rate constants in logarithmic scale in the range $-2 \leqslant \log_{10}(k_{ij}^0)/\log_{10}(k_{ij}^{0R}) \leqslant 2$ ($ij = 12, 21, 23, 32, 31$) with a sampling interval of 0.1 (k_{13}^0 is imposed by detailed balance). The resonant dynamical parameters are $\lambda_+^R = -0.784 \text{ s}^{-1}$, $\lambda_-^R = -20.756 \text{ s}^{-1}$, $\theta_+^R = 1.659$ rad, and $\theta_-^R = -0.025$ rad. The figure is given for the following standard enthalpies of reaction: $\Delta_{12}H^0/RT^0 = 5$, $\Delta_{23}H^0/RT^0 = -10$, $\Delta_{31}H^0 = -\Delta_{12}H^0 - \Delta_{23}H^0$. The vertical dashed line gives the targeted value θ_-^R of the eigenangle.

Now, for $\theta_\pm = \theta_\pm^R$, the response function, given in Eq. (29), is

$$R(\lambda_\pm, E^0, \theta_\pm = \theta_\pm^R) = \left| \alpha_+ \frac{\lambda_+ \lambda_+^R}{(\lambda_+^R)^2 + \lambda_+^2} \right| \left| \alpha_- \frac{\lambda_- \lambda_-^R}{(\lambda_-^R)^2 + \lambda_-^2} \right|, \tag{33}$$

where the coefficients $\alpha_\pm$ are deduced from Eq. (20) for $\theta_\pm = \theta_\pm^R$. The response $R(\lambda_\pm, E^0, \theta_\pm = \theta_\pm^R)$ is the product of a Lorentzian function in λ_+ and another one in λ_-. Therefore, it possesses an exact maximum for $\lambda_\pm = \lambda_\pm^R$. We compare these analytical, approximate results with the exact, numerical approach. Figure 3 represents the function $R(\lambda_\pm, E^0, \theta_\pm)$ de-
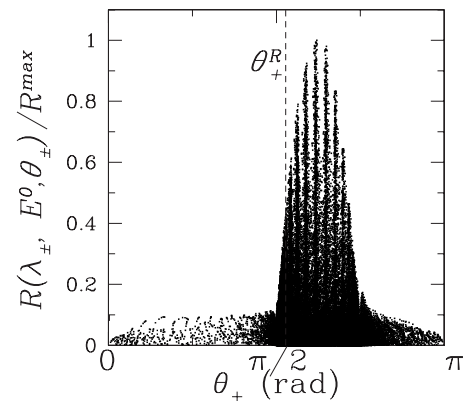

FIG. 2. Normalized response $R(\lambda_\pm, E^0, \theta_\pm)/R^{\max}$ versus eigenangle θ_+ for enzymatic networks with three states. Same parameter values as in Fig. 1 with Eq. (9) to compute θ_+ from the rate constant sampling. The vertical dashed line gives the targeted value θ_+^R.
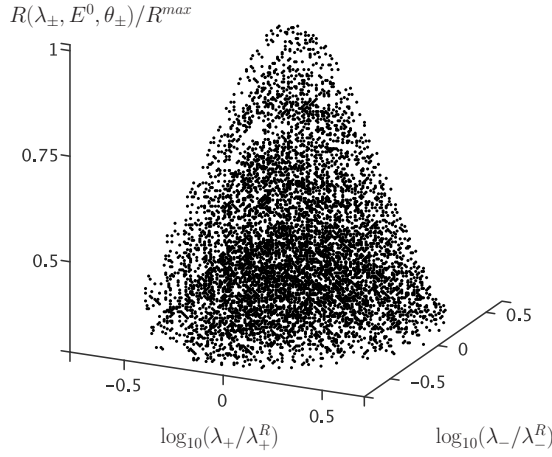
$R(\lambda_\pm, E^0, \theta_\pm)/R^{max}$

FIG. 3. Normalized response $R(\lambda_\pm, E^0, \theta_\pm)/R^{max}$ versus normalized eigenvalues in logarithmic scale, $\log_{10}(\lambda_+/\lambda_+^R)$, $\log_{10}(\lambda_-/\lambda_-^R)$, for enzymatic networks with three states. Same parameter values as in Fig. 1 with Eq. (7) to compute $\lambda_\pm$ from the rate constant sampling.

fined in Eq. (29) versus the two real eigenvalues (λ_+, λ_-) for the set of generated enzymatic networks. As expected,

$R(\lambda_\pm, E^0, \theta_\pm)$ displays a maximum for $\lambda_\pm^{max} \approx \lambda_\pm^R$. For all the chosen values of the targeted dynamical parameters $(\theta_\pm^R, \lambda_\pm^R)$, we obtain a good agreement between $\lambda_\pm^{max}$ and $\lambda_\pm^R$ in the eigenvalue space. Figure 3 is a projection of the five-variable function $R(\lambda_\pm, E^0, \theta_\pm)$ on a two-dimensional space, so that the points are not located on a surface but form a cloud.

The targeted dynamical parameters $(\lambda_\pm^R, \theta_\pm^R)$ define a family of enzymatic networks whose equilibrium state $\mathcal{E} = \binom{E^0}{ES^0}$ obeys Eq. (10) for $\theta_\pm = \theta_\pm^R$. We use Eq. (33) and the expression of the coefficients $\alpha_\pm$ given in Eq. (20) for $(\lambda_\pm = \lambda_\pm^R, \theta_\pm = \theta_\pm^R)$, to determine the response function

$$R^R(E^0) = R(\lambda_\pm = \lambda_\pm^R, E^0, \theta_\pm = \theta_\pm^R) = E^0 ES^0 EP^0 C(\theta_\pm^R), \tag{34}$$

where $ES^0 = \frac{1}{2}\{1 + E^0[\tan(\theta_+^R) + \tan(\theta_-^R)] \pm \sqrt{\Delta(E^0)}\}$ with

$$\Delta(E^0) = \{1 + E^0[\tan(\theta_+^R) + \tan(\theta_-^R)]\}^2 + 4E^0(1 - E^0)\tan(\theta_+^R)\tan(\theta_-^R)$$

and $EP^0 = 1 - E^0 - ES^0$. The constant term is given by

$$C(\theta_\pm^R) = \frac{\left\{\tan(\theta_+^R)\dfrac{\Delta_{12}H^0}{RT^0} + [1 + \tan(\theta_+^R)]\dfrac{\Delta_{31}H^0}{RT^0}\right\}\left\{\tan(\theta_-^R)\dfrac{\Delta_{12}H^0}{RT^0} + [1 + \tan(\theta_-^R)]\dfrac{\Delta_{31}H^0}{RT^0}\right\}}{4\cos(\theta_+^R)\cos(\theta_-^R)[\tan(\theta_+^R) - \tan(\theta_-^R)]^2}. \tag{35}$$

Although we did not build $R(\lambda_\pm, E^0, \theta_\pm)$ in this goal, the function $R^R(E^0)$ reaches a maximum for a concentration E^{max} that can be determined from the following equation:

$$\begin{aligned}\sqrt{\Delta(E^{max})}&\{[1 + \tan(\theta_+^R) + \tan(\theta_-^R)]\{2 + 3E^{max}[\tan(\theta_+^R) \\ &+ \tan(\theta_-^R)] + 2\tan(\theta_+^R)\tan(\theta_-^R)(2 - 3E^{max})\} \\ &= \pm[1 + \tan(\theta_+^R) + \tan(\theta_-^R)] \\ &\times\left(2\Delta(E^{max}) + \frac{E^{max}}{2}\frac{d\Delta}{dE^0}(E^{max})\right).\end{aligned} \tag{36}$$

In general, E^{max} differs from the equilibrium state E^{0R} associated with the resonant set of rate constants $(k_{12}^{0,R}, k_{21}^{0,R}, k_{23}^{0,R}, k_{32}^{0,R}, k_{31}^{0,R})$. As seen in Fig. 4, $R^R(E^0)$ possesses a maximum

$$R^{max} = R^R(E^{max}) \tag{37}$$

which is reached for the predicted value E^{max} that is implicitly defined in Eq. (36). Note that if $E^0 = 0$ or $E^0 = 1$, the function vanishes and the network is associated with an $A \rightleftharpoons B$ type degenerate mechanism instead of the triangular mechanism of Eq. (2).

In conclusion of this section, the designed response function $R(\lambda_\pm, E^0, \theta_\pm)$ possesses a single maximum for the enzymatic network whose dynamics is characterized by $(\lambda_\pm^R, E^{max}, \theta_\pm^R)$. In the next section, we apply the designed resonance phenomenon associated with $(\lambda_\pm^R, E^0, \theta_\pm^R)$, for any value of the equilibrium concentration E^0, to the screening of a large set of enzymatic networks, which are all associated with the same equilibrium. The choice of the targeted dynamical parameters $\lambda_\pm^R, \theta_\pm^R$ as the resonant set for the function $R(\lambda_\pm, E^0, \theta_\pm)$, will enable us to identify the enzymatic network, whose dynamical parameters are the closest to $\lambda_\pm^R, \theta_\pm^R$.

V. APPLICATION TO SCREENING AND IDENTIFICATION OF A TARGETED DYNAMICS

Significant advances have been made in the development of NMR methods for studying biomolecular dynamics [28]. NMR spectra of amino acids located in known position can be used as markers for the conformation of the enzyme in the presence and absence of the substrate [29–31], so that the states E and ES can be distinctly observed. Moreover, NMR methods are compatible with temperature variation. The development of microfluidics makes us confident in the genera-
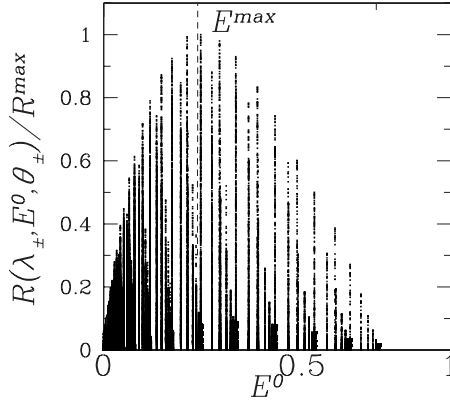
FIG. 4. Normalized response $R(\lambda_\pm, E^0, \theta_\pm)/R^{max}$ versus equilibrium concentration E^0 for enzymatic networks with three states. Same parameter values as in Fig. 1. The vertical dashed line gives the implicit analytical prediction for E^{max} deduced from Eq. (36).

tion of temperature oscillations whose frequency can reach 10^5 Hz in microreactors of about 50 μm size [32,33]. It is thus possible to observe a large range of chemical relaxation times, from 10^{-5} s to a few seconds, which cover the characteristic times of the fast conformational exchanges of enzymes [30,31]. For typical enthalpies of reaction $\Delta_{ij}H^0$ around 10 kcal mol^{-1} [28] at $T^0 = 310$ K, the order of magnitude of $\beta E^1_{cos}(|\lambda^R_\pm|)$ or $\beta ES^1_{cos}(|\lambda^R_\pm|)$ reaches 1% of the equilibrium concentrations (E^0, ES^0) for amplitudes of temperature oscillations $\beta T^0 \simeq 0.5$ K. Filtering at the appropriate frequencies and complex Fourier transform should make easy the determination of the out-of-phase amplitudes of the concentrations. These techniques could be used to experimentally determine the values of the response function for many three-state enzymatic networks.

We consider a set of enzymatic networks with unknown rate constants k^0_{ij} and we wish to identify the one which has the targeted values k^{0R}_{ij}. By "a set of networks," we do not mean a mixture of all the enzymatic networks to be screened, but many tubes each containing substrate S and product P to the same known concentrations and a single enzymatic network $\{E, ES, EP\}$ with unknown rate constants. The targeted equilibrium state is denoted by (E^0, ES^0). The equilibrium states and the enthalpies of reaction $\Delta_{ij}H^0$ at temperature T^0 of each enzymatic network can be easily determined by standard methods and all the tubes with networks which are not associated with (E^0, ES^0) can be disregarded. The dynamics of the network in each remaining tube is characterized by three rate constants, for example, k^0_{12}, k^0_{23}, and k^0_{31}. The three other rate constants are imposed by detailed balance and are given by $k^0_{21} = E^0 k^0_{12}/ES^0$, $k^0_{32} = ES^0 k^0_{23}/(1 - E^0 - ES^0)$, and $k^0_{13} = (1 - E^0 - ES^0)k^0_{31}/E^0$. Equivalently, each network is associated with three dynamical parameters $(\lambda_\pm, \theta_+)$ and the value of the eigenangle θ_- is imposed by detailed balance according to Eq. (10).

In order to find the enzymatic network whose parameter values are the closest to the targeted ones $(\lambda^R_\pm, \theta^R_+)$, we suggest the experimentalists to follow this protocol. Each tube is submitted to the same two-frequency temperature modulation at $|\lambda^R_+|$ and $|\lambda^R_-|$, as defined in Eq. (24). The two oscillating concentrations $[E(t), ES(t)]$ in each tube are collected,
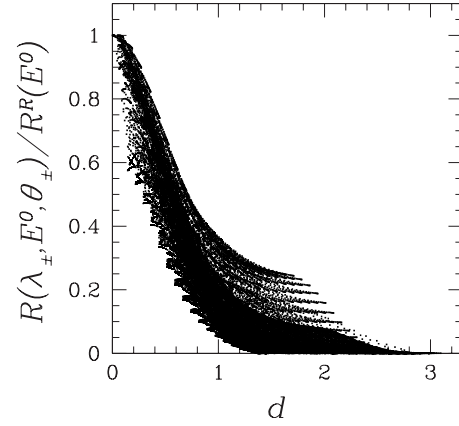

FIG. 5. Normalized response $R(\lambda_\pm, E^0, \theta_\pm)/R^R(E^0)$ versus the distance d for enzymatic networks with the same equilibrium state $(E^0 = 0.741, ES^0 = 0.185)$. The figure is plotted by using Eqs. (29), (34), and (38) to compute the response function and the distance d from a uniform sampling of three rate constants in logarithmic scale in the range $-2 \leqslant \log_{10}(k^0_{ij})/\log_{10}(k^{0R}_{ij}) \leqslant 2$ $(i, j = 12, 23, 31)$ with a sampling interval of 0.1. The three other rate constants are imposed by detailed balance. The targeted dynamical parameters are $(\lambda^R_+ = -0.246$ s^{-1}, $\lambda^R_- = -2.484$ s^{-1}, $\theta^R_+ = -0.781$ rad). The value of θ^R_- is deduced from Eq. (10). The enthalpies of reaction are the same as in Fig. 1.

thanks to NMR spectra for example. The first-order out-of-phase amplitudes $[E^1_{cos}(|\lambda^R_\pm|), ES^1_{cos}(|\lambda^R_\pm|)]$ are extracted from the global signal thanks to Fourier transform. Then, Eq. (28) is used to build the value of the response function $R(\lambda_\pm, E^0, \theta_\pm)$ associated with each tube, i.e., with each enzymatic network. The resonant value $R^R(E^0)$ of the function is analytically calculated by using Eq. (34). Finally, the values of the normalized response function $R(\lambda_\pm, E^0, \theta_\pm)/R^R(E^0)$ are computed for each tube. According to the results of Sec. IV, for fixed values of the equilibrium concentrations (E^0, ES^0), the response function $R(\lambda_\pm, E^0, \theta_\pm)$ is maximum for the resonant enzymatic network characterized by $(\lambda^R_\pm, \theta^R_+)$. The closeness of the ratio $R(\lambda_\pm, E^0, \theta_\pm)/R^R(E^0)$ of an unknown network to 1 induces the closeness of its dynamical parameters $(\lambda_\pm, \theta_+)$ to the resonant ones $(\lambda^R_\pm, \theta^R_+)$. The method enables us to find out the tube which contains the enzymatic network whose dynamical parameters are the closest to the desired ones.

In order to quantify the difference between the dynamical parameters $(\lambda_+, \lambda_-, \theta_+)$ of an unknown enzyme and the targeted values $(\lambda^R_+, \lambda^R_-, \theta^R_+)$, we introduce the following distance:

$$d = \frac{1}{3}\left(\left| \log_{10}\left(\frac{\lambda_+}{\lambda^R_+}\right) \right| + \left| \log_{10}\left(\frac{\lambda_-}{\lambda^R_-}\right) \right| + \left| \log_{10}\left| \frac{\tan(\theta_+)}{\tan(\theta^R_+)} \right| \right| \right).$$
(38)

Figure 5 represents the normalized response function $R(\lambda_\pm, E^0, \theta_\pm)/R^R(E^0)$ versus the distance d for a sampling of the rate constants k^0_{12}, k^0_{23}, and k^0_{31}. Each value of the ratio can be related to a maximum distance. For example, if the set contains an enzyme E^T (with T for target) such that $R^T(\lambda_\pm, E^0, \theta_\pm)/R^R(E^0) > 0.8$, then, we deduce from Fig. 5

TABLE IV. Closeness of the dynamical parameter values to the resonant values does not mean closeness of the rate constants to the corresponding resonant values. The four first lines give the equilibrium state and the dynamical parameters of the resonant enzymatic network and a network which is associated with a distance $d = 0.2$ to the resonant network. The second eigenangle value θ_-^R or θ_- is deduced from the other parameters and detailed balance. The four last lines give the rate constant values which are associated with these two networks. The expression of the rate constants versus the eigenvalues and eigenangles that is given in Table II is used to compute the eighth line from the fourth line.

E^0	ES^0	λ_+^R	λ_-^R	θ_+^R (rad)	θ_-^R (rad)
0.741	0.185	-0.246	-2.484	2.361	0.274
E^0	ES^0	λ_+	λ_-	θ_+ (rad)	θ_- (rad)
0.741	0.185	-0.672	-2.228	2.787	0.623
k_{12}^{0R}	k_{21}^{0R}	k_{23}^{0R}	k_{32}^{0R}	k_{31}^{0R}	k_{13}^{0R}
0.010	0.040	0.200	0.500	1.800	0.180
k_{12}^0	k_{21}^0	k_{23}^0	k_{32}^0	k_{31}^0	k_{13}^0
0.398	1.592	0.252	0.629	0.072	0.007

that $d < 0.4$, i.e., that the dynamical parameters of E^T differ from the resonant values $[\lambda_\pm^R, \tan(\theta_+^R)]$ by less than a factor $f = 2.5$ in average. With respect to standard dynamical parameter determination in biochemistry, this result is satisfying. Then, the analytical expression of the rate constants versus the eigenvalues, eigenangles and equilibrium state given in Table II can be used to determine the rate constant values associated with E^T. However, the nonlinear dependence of the rate constants on the dynamical parameters $(\lambda_\pm, \theta_+)$ is at the origin of a larger error on the rate constants than on the eigenvalues and eigenangle. In particular, a small variation of the angle θ_+ may induce a large variation of its tangent and consequently of the rate constants. The precision on the k_{ij}^0 determination strongly depends on the equilibrium concentrations. In Table. IV, we give an example of enzymatic network such that $d = 0.2$ and $R(\lambda_\pm, E^0, \theta_\pm)/R^R(E^0) = 0.85$. The worst result is obtained for λ_+, which differs by less than a factor of 3 from the resonant value. However, the rate constants k_{12}^0 and k_{21}^0 differ by a factor 40 from the corresponding resonant values.

Note that the screening procedure we propose does not require any frequency sweep. To summarize the experimental protocol, each tube containing a given enzymatic network is submitted to the targeted modulations at $|\lambda_\pm^R|$, the out-of-phase amplitudes of the concentration oscillations are measured, the resonant value $R^R(E^0)$ of the function is analytically computed using Eq. (34) and the value of the normalized response function $R(\lambda_\pm, E^0, \theta_\pm)/R^R(E^0)$ is built using Eq. (28) for each sample tube. Finally, the resonant values $(\lambda_\pm^R, \theta_+^R)$ of the dynamical parameters are allocated to the enzymatic network, such that the ratio $R(\lambda_\pm, E^0, \theta_\pm)/R^R(E^0)$ is the closest to 1. The value of this ratio determines the accuracy of the dynamical parameter determination.

VI. CONCLUSION

We propose a method for the screening of three-state enzymatic networks, which is based on the resonant response of a biological medium to temperature modulations. This approach to biochemical dynamics enables us to identify the enzyme associated with a targeted dynamics and to assess the precision on the determination of all its rate constants without resorting to a fit. The experimental validation requires temperature oscillations at the characteristic chemical frequencies and the specific detection of the different conformational enzymatic states. The *in vitro* validation looks realistic if we consider the recent advances in microtechnologies and in spectroscopies of biological species such as NMR. Information retrieval is noninvasive and recent progress in Raman scattering microscopy give opportunity to probe biochemical reactions in living cells [34]. Our method could be contemplated for the *in vivo* characterization of biological medium dynamics.

[1] P. M. Hwang, W.-Y. Choy, E. I. Lo, L. Chen, J. D. Forman-Kay, C. R. H. Raetz, G. G. Privé, R. E. Bishop, and L. E. Kay, Proc. Natl. Acad. Sci. U.S.A. **99**, 13560 (2002).

[2] J. K. Yano, M. R. Wester, G. A. Schoch, K. J. Griffin, C. D. Stout, and E. F. Johnson, J. Biol. Chem. **279**, 38091 (2004).

[3] J. Gao and D. G. Truhlar, Annu. Rev. Phys. Chem. **53**, 467 (2002).

[4] R. Breslow, Acc. Chem. Res. **28**, 146 (1995).

[5] W. Vance, A. Arkin, and J. Ross, Proc. Natl. Acad. Sci. U.S.A. **99**, 5816 (2002).

[6] J. Ross, Acc. Chem. Res. **36**, 839 (2003).

[7] A. S. Torralba, K. Yu, P. Shen, P. J. Oefner, and J. Ross, Proc. Natl. Acad. Sci. U.S.A. **100**, 1494 (2003).

[8] H. Qian, J. Phys. Chem. B **110**, 15063 (2006).

[9] M. Eigen and L. DeMayer, in *Techniques of Organic Chemistry* (Wiley Interscience, New York, 1963), Vol. 8, Pt. II.

[10] E. L. Elson and D. Magde, Biopolymers **13**, 1 (1974).

[11] D. Magde, E. L. Elson, and W. W. Webb, Biopolymers **13**, 29 (1974).

[12] H. Qian and E. L. Elson, Proc. Natl. Acad. Sci. U.S.A. **101**, 2828 (2004).

[13] S. Charier, A. Meglio, D. Alcor, E. Cogné-Laage, J.-F. Allemand, L. Jullien, and A. Lemarchand, J. Am. Chem. Soc. **127**, 15491 (2005).

[14] A. E. Kamholz, B. H. Weigl, B. A. Finlayson, and P. Yager, Anal. Chem. **71**, 5340 (1999).

[15] C. G Moles, P. Mendes, and J. R. Banga, Genome Res. **13**, 2467 (2003).

[16] A. V. Karnaukhov, E. V. Karnaukhova, and J. R. Williamson, Biophys. J. **92**, 3459 (2007).

[17] J. T. Mettetal, D. Muzzey, C. Gomez-Uribe, and C. van Oude-naarden, Science **319**, 482 (2008).

[18] H. Berthoumieux, L. Jullien, and A. Lemarchand, Phys. Rev. E **76**, 056112 (2007).

[19] L. Jullien, A. Lemarchand, and H. Lemarchand, J. Chem. Phys. **112**, 8293 (2000).

[20] D. Alcor, V. Croquette, L. Jullien, and A. Lemarchand, Proc. Natl. Acad. Sci. U.S.A. **101**, 8276 (2004).

[21] L. Jullien and A. Lemarchand, J. Phys. Chem. B **105**, 4415 (2001).

[22] H. Berthoumieux, L. Jullien, and A. Lemarchand, J. Phys. Chem. B **111**, 2045 (2007).

[23] J. Wei and C. D. Prater, Adv. Catal. **13**, 203 (1962).

[24] Y. Chen, Adv. Chem. Phys. **37**, 67 (1978).

[25] H. A. Kramers, Physica (Amsterdam) **7**, 284 (1940).

[26] S. Glasstone, K. J. Laidler, and H. Eyring, *The Theory of Rate Processes: The Kinetics of Chemical Reactions, Viscosity, Diffusion and Electrochemical Phenomena* (McGraw-Hill, New York, 1941).

[27] T. L. Hill, Proc. Natl. Acad. Sci. U.S.A. **73**, 679 (1976).

[28] M. Akke, Curr. Opin. Struct. Biol. **12**, 642 (2002).

[29] S. Rozovsky, G. Jogl, L. Tong, and A. E. McDermott, J. Mol. Biol. **310**, 271 (2001).

[30] L. Wang, Y. Pang, T. Holder, J. R. Brender, A. V. Kurochkin, and E. R. P. Zuiderweg, Proc. Natl. Acad. Sci. U.S.A. **98**, 7684 (2001).

[31] R. Cole and J. P. Loria, Biochemistry **41**, 6072 (2002).

[32] D. Braun and A. Libchaber, Appl. Phys. Lett. **83**, 5554 (2003).

[33] S. Duhr and D. Braun, Proc. Natl. Acad. Sci. U.S.A. **103**, 19678 (2006).

[34] X. S. Xie, J. Yu, and W. Y. Yang, Science **312**, 228 (2006).